

# INTERNATIONAL SOCIETY FOR SOIL MECHANICS AND GEOTECHNICAL ENGINEERING



*This paper was downloaded from the Online Library of the International Society for Soil Mechanics and Geotechnical Engineering (ISSMGE). The library is available here:*

<https://www.issmge.org/publications/online-library>

*This is an open-access database that archives thousands of papers published under the Auspices of the ISSMGE and maintained by the Innovation and Development Committee of ISSMGE.*

# Numerical simulation of a tunnel excavated in a porous collapsible soil

M. M. Farias & A. P. Assis  
*University of Brasilia, Brazil*

**ABSTRACT:** During tunnelling excavations of the Brasilia subway, excessive surface settlements were observed. The settlement profile along the tunnel symmetry axis is not typical, increasing its value from the tunnel crown to the surface. This behaviour is controlled by a thick layer of a porous and collapsible soil, which is common in the central part of Brazil. The main mechanical characteristic of this soil is that it may present a structural collapse when is either saturated or subjected to stress state changes. This paper presents a numerical simulation of a cross-section, where the thickness of this clay layer reaches up to 40 m. The tunnelling excavation was instrumented by superficial topographic marks, extensometers and convergence pins. A Finite Element Program was used for simulating the excavation under plane strain conditions. A modified version of the Cam-Clay Model was adopted to represent the soil behaviour. The results show an excellent agreement between the observed and predicted settlements as well as that the collapsible behaviour of the soil must be considered. The numerical results also indicate that the collapse criterion, in this case, is associated with an extension zone on the upper surroundings of the tunnel which is induced by tunnelling excavation.

## 1 INTRODUCTION

Underground works modify significantly the stress state around the opening and consequently induce deformations in the tunnel influence zone. The size and magnitude of the induced deformation field depend upon several parameters such as in-situ stress, tunnel depth, opening size and shape, deformability and strength of the ground and support, and the ground-support interaction. For shallow tunnels in soils, the induced deformation and displacement fields play an important role, because they affect the zone where the public utilities and foundations are located, which can be severely damaged by tunnelling excavation. This paper aims to evaluate the deformation and displacement fields of a tunnel excavated in a porous collapsible soil.

## 2 THE BRASILIA SUBWAY

The Brasilia Subway has been under construction since 1992. Line 1 is of 40 km long, including a tunnel, 6.8 km long, 9.6 m of diameter, 15 m deep, excavated by the New Austrian Tunnelling Method (NATM). The local geology indicates the presence of a thick layer of porous red clay, overlying residual soils of slate and metarhytmite. Between stations PP-2

and PP-3, the porous clay layer reaches up to 40 m of thickness and the water table is not present. This portion was selected as a typical cross-section in this paper, because the tunnel influence zone is confined within the porous red clay. This simplifies the problem and its boundary conditions, besides giving a better understanding of the structural collapse effect on the displacement field. In most cases, the observed surface settlements were greater than the tunnel crown convergence, which is typical for collapsible soils.

## 3 INSTRUMENTATION

For this analysis, a complete instrumented cross-section (S-4294), between stations PP-2 and PP-3, was chosen, far away from other interferences such as soil improvement, tunnel portal, roads etc. It has five surface topographic marks, two extensometers and seven convergence pins (Figure 1). The surface settlement subsidence (Figure 2) was obtained from the topographic mark measurements by a curve fitting technique, using a gaussian curve as suggested by Peck (1969). The settlement profile along the tunnel symmetry axis was obtained using the measurements from the topographic mark M1, the two extensometers (E1, E2) and the convergence pin

P1 (Figure 3). As the convergence pin P1 measures only part of the total convergence, a correction was made. For simplicity, the method recommended by Cording & Hansmire (1975) was used, considering the data from the nearest extensometer E2 and a volume change equal to zero.

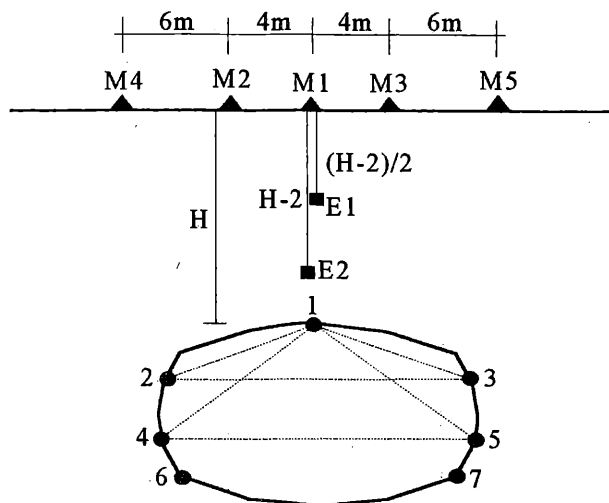


Figure 1. Typical instrumentation.

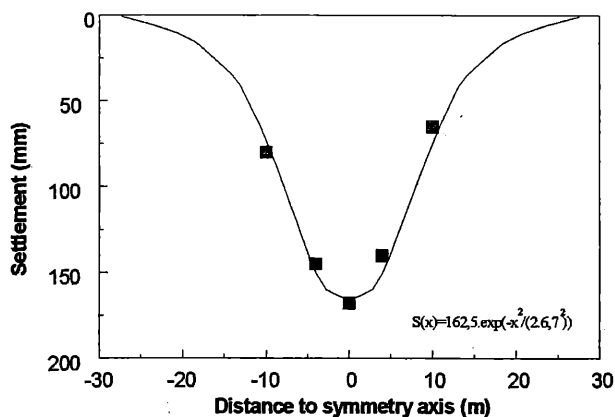


Figure 2. Surface settlement subsidence.

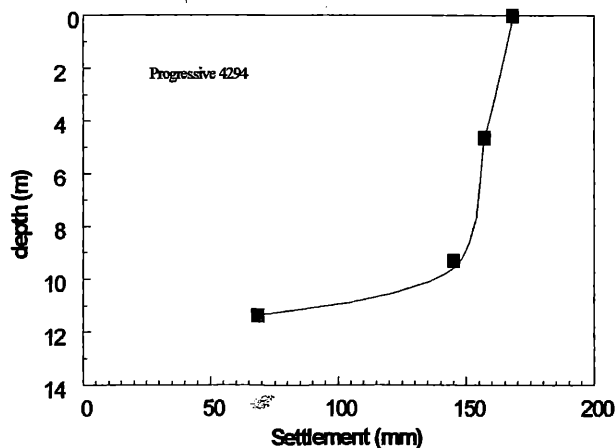


Figure 3. Settlement profile along the symmetry axis.

The settlement profile shows an enormous increase of these values, from 68 mm at the tunnel crown to 168 mm at the surface. This behaviour, where the settlements increase towards the surface, is not common. It indicates another source of displacements between the tunnel and ground surface. This source of displacements is related to the collapsible properties of some porous soils, which justifies a numerical analysis of the tunnel behaviour under these circumstances.

#### 4 NUMERICAL SIMULATION

In this analysis, the Finite Element Program ALLFINE, developed by Farias (1993), was used. The program has an extensive list of options, including several element types and loading conditions. It can simulate static analyses in terms of either total or effective stress and also transient analyses with coupled consolidation. Four constitutive models are available: anisotropic linear elastic, non-linear elastic (K-G model), modified Cam-Clay and a new version of the modified Cam-Clay. The program has an automatic algorithm for determining increment sizes of load or time. Several solution schemes of non-linear equations are implemented. The program allows the simulation of underground structures, excavated in one or more stages, including or not structural collapse.

The adopted constitutive model is a new version of the Modified Cam-Clay Model, proposed by Naylor (1994) and implemented by Farias (1993). It includes a tension zone and a flattening of the yielding surface (Figure 4).

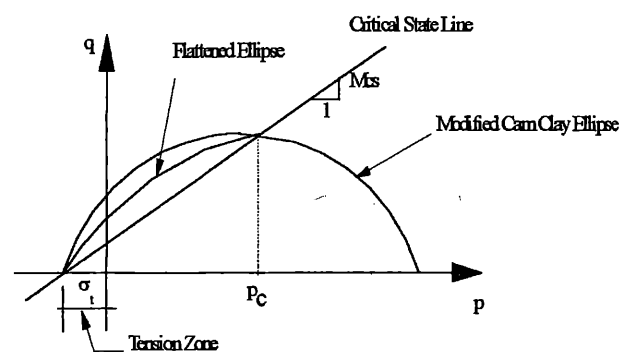


Figure 4. Critical state model.

Two ellipses are used as yielding surfaces. In the normally consolidated zone, the ellipse is the same as in the Modified Cam-Clay Model. In the over-consolidated zone, a new ellipse is introduced. It can change from the original one to the critical state line, according to the flattening parameter  $k$  which ranges from 0 to 1. The tension zone is represented by the

parameter  $\sigma_t$  which is defined by the ratio between the critical state cohesion and the tangent of the critical state friction angle. Usually this cohesion is zero, but a small value helps to overcome numerical problems when the stress values are very small. Other parameters are the unloading/reloading elastic modulus, Poisson's ratio and the plastic bulk modulus  $\chi=(\lambda-\kappa)/(1+e_0)$  as defined by Naylor *et al.* (1981). The in-situ and over-consolidation stresses are also given.

The tunnelling excavation is simulated as shown in Figure 5. The initial stresses  $\sigma_0$  were calculated considering a geostatic stress state with unit weight equal to 16 kN/m<sup>3</sup> and a coefficient of earth-pressure at rest  $K_0$  equal to 0.6. Stresses in the elements to be excavated are set to zero, generating a state of stress  $\sigma_0^*$ . The total force  $F$  applied to the tunnel surface is given by:

$$F = \int_V \mathbf{B}^T (\sigma_0 - \sigma_0^*) dV \quad (1)$$

where  $\mathbf{B}$  is the deformation-displacement matrix.

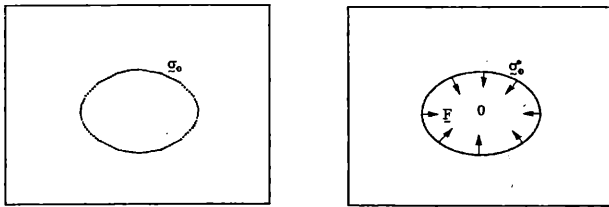


Figure 5. Numerical simulation of tunnel excavation.

Collapse settlements were simulated according to a method similar to that described by Nobari and Duncan (1972). Two material properties sets must be defined: (A) relating to conditions before collapse and (B) describing the material behaviour after collapse. The simulation follows three stages as illustrated in Figure 6(a). An element with properties (A) is initially loaded up to the stress point  $\sigma^A$ . The stress point is then moved to  $\sigma^B$  under restrained conditions. Finally the load due to the stress difference

$$F = \int_V \mathbf{B}^T (\sigma^A - \sigma^B) dV \quad (2)$$

is computed and applied to the element with properties (B), reaching a new equilibrium condition at stress point  $\sigma^C$ .

To determine the stress point  $\sigma^B$  under restrained conditions Nobari and Duncan proposed the following methodology: (1) load the material with

properties (A) along stress path OPA in Figure 6(b) and compute the correspondent strain path; (2) impose the computed strain path to the material with new property set (B) to find stress point  $\sigma^B$ . The proposed stress path is closed related to Nobari and Duncan's experiments and to the hyperbolic constitutive model of Duncan and Chang (1970).

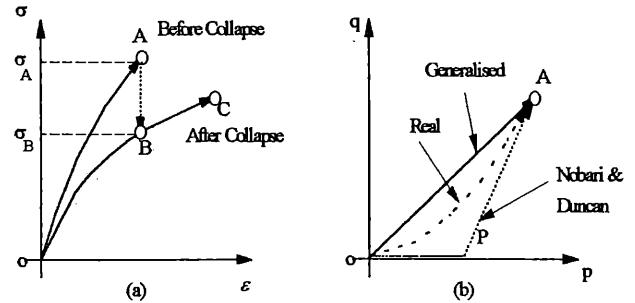


Figure 6. Simulation of collapse.

More recently, Naylor *et al.* (1989) proposed a so called "generalised path" linking the origin O to point A in the stress space shown in Figure 6(b). The method was successfully applied to a backanalysis of Beliche Dam in Portugal (Tong, 1992) using the linear elastic and the non-linear elastic K-G model. However they were not successful to apply it to the same problem with the critical state model used here. Farias (1993) proposed and implemented the use of the "real effective stress path" as computed from the finite element analysis up to collapse point  $\sigma^A$ . This method has the advantage of being model independent and extremely easy to implement. It has been successfully applied with the critical state model (Naylor *et al.*, 1993). The stress path used in the three methods described above are simply an artifice to compute stress point  $\sigma^B$  and do not necessarily relate to the physical path followed by the material. However, numerical studies carried out by Maranhã (1992) show that the position of the stress point  $\sigma^B$  is not strongly sensitive to the stress path adopted between points O and A.

The described collapse settlement scheme was originally proposed to simulate collapse due to saturation, but can be used to compute structural collapse due to any other causes, such as excessive stress or deformation changes.

## 5 RESULTS

The finite element mesh is shown in Figure 7. It has 706 nodes and 225 elements (15 isoparametric triangles with 6 nodes and 210 isoparametric elements with 8 nodes). The tunnel is represented by a circular cross-section with an equivalent radius of

4.61 m and an overburden of 11.3 m. Table 1 presents a summary of the soil properties. A small tension zone was adopted. The over-consolidation ratio was set to 1.5 and the Poisson's ratio to 0.3. The critical state friction angle was considered equal to the peak friction angle obtained from several in-situ and laboratory tests (Ortigão & Macedo, 1994). The deformability parameters were obtained from a parametric analysis where the observed displacements were matched.

Table 1. Material properties.

sets	E (kPa)	$\nu$	$\phi_{cs}$	$\chi$
A	25.000	0,3	28°	0,002
B	5.000	0,3	28°	0,010

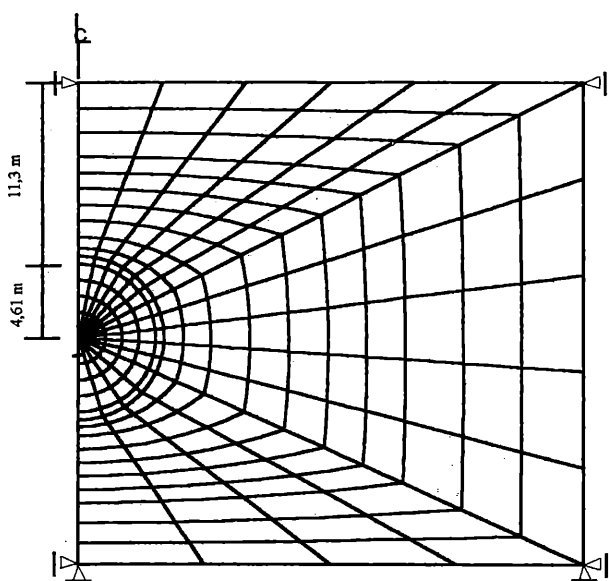


Figure 7. Initial finite element mesh.

The analysis was carried out in two stages. In the first stage, the unloading due to tunnelling excavation was simulated and in the second one, collapse was applied to some elements. In the first stage, the analysis was carried out up to the tunnel failure, which occurred for a relief of 75% of the original stress. The ground reaction curve (convergence versus support pressure) is presented in Figure 8. The final convergence, after the support has been mobilised, was around 68 mm, which corresponds to a relief of 62% of the original stresses. The horizontal and vertical stress distribution after 62% of stress relief are presented in Figures 9 and 10, respectively. It can be noticed that there is a horizontal stress concentration and a vertical stress relief in the collapsible zone above the tunnel. The contrary occurs in the spring line of the tunnel.

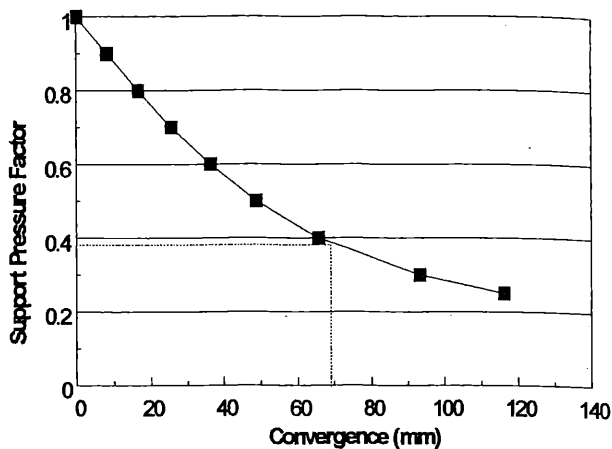


Figure 8. Ground reaction curve.

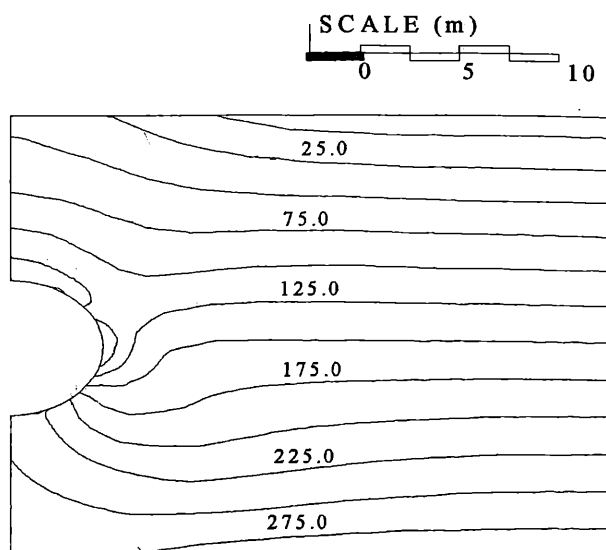


Figure 9. Horizontal stress distribution.

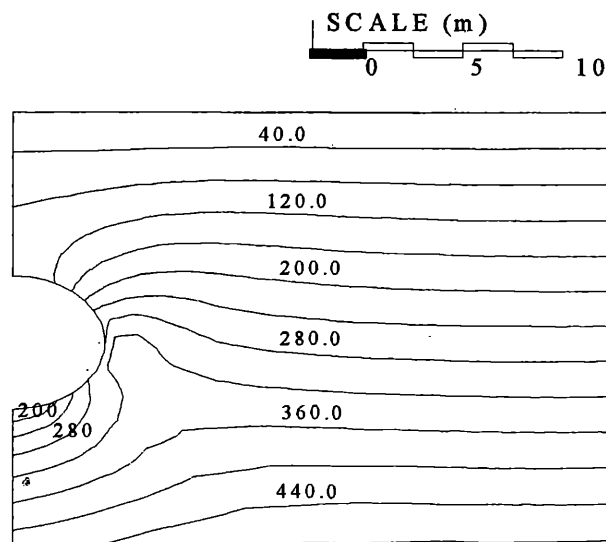


Figure 10. Vertical stress distribution.

The main difficulty in the second stage was to determine which elements should be subjected to collapse. Laboratory results demonstrate that the collapse potential of this porous soil decreases with the depth and is practically negligible at 8 m. Instrumentation data clearly indicate that collapse has occurred in the elements above the tunnel. The measured settlement in extensometer E2 (Figure 3) suggests that the collapse zone is somewhat deeper than that indicated by the laboratory tests. A parametric analysis was done to determine the parameters that affect mostly the soil collapse. It was concluded that settlements were significantly affected by the elastic modulus, plastic bulk modulus and extension of the collapsible zone. The parameters that yielded the best agreement between observed and predicted values are those reported in Table 1. The parametric study also indicate that the extension of the collapsible zone goes between the second and third columns of elements down to a depth of 8 m to the tunnel crown.

The stress state previous to collapse was intensively investigated aiming to find a structural collapse criterion based on stress level. It was frustrated and no apparent correlation between stress state and collapse zone could be established. A better hint came out when some deformation graphs were plotted. The vertical deformation plots showed a zone, above the tunnel, subjected to extension (Figure 11). This zone coincides to that one already obtained by the parametric analysis. The weak cementation links of the porous clay apparently do not resist extension strains, leading to the collapse of its structure.

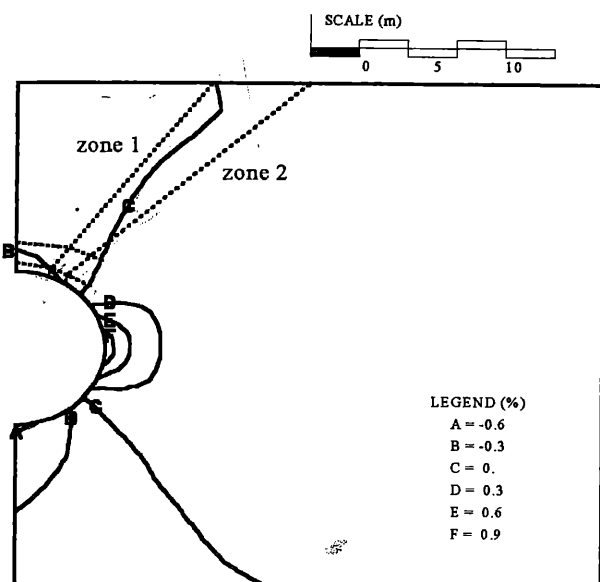


Figure 11. Vertical deformation.

Two collapse zone extension were studied (Figure 11). Zone 1 includes the two element columns and goes up to 8 m deep. Zone 2 extends further and reaches 10 m deep, including the elements of the third column. Figure 12 shows a comparison between the settlement subsidence obtained for the two collapse zones and the measured values from the topographic marks. Also, settlements previous to collapse are plotted. The predicted settlements and the shape of the subsidence curves are in excellent agreement with the observed values. The values from the topographic mark M5 indicate that the collapse zone is a little more extensive than that adopted (Figure 11).

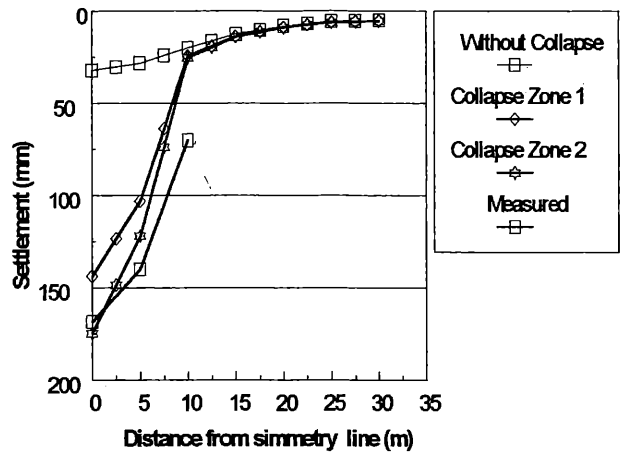


Figure 12. Comparison of settlement subsidence.

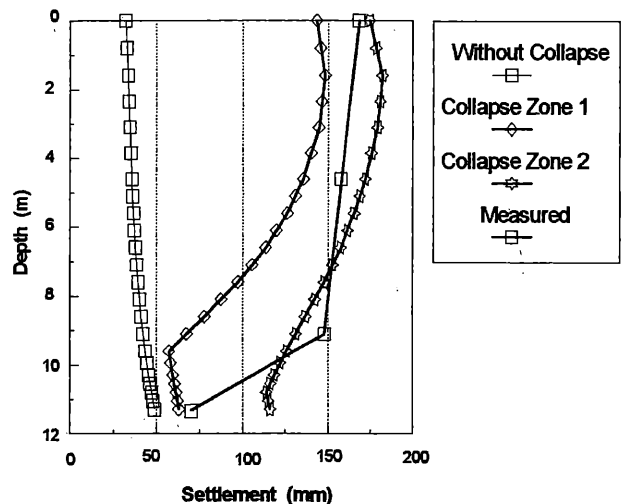


Figure 13. Comparison of settlement profiles.

Figure 13 shows the comparison between the observed and predicted settlement profiles along the tunnel symmetry axis. Again, the results are in good agreement, except in the zone closest to the tunnel crown. The method of Cording & Hansmire (1975)

used to correct the measured settlement of the convergence pin P1 does not account for the collapse volume change between extensometer E2 and the tunnel crown. If this volume change were considered, a better agreement would have been achieved. The settlement profile without considering soil collapse shows the values increasing with depth, as expected. These results reinforce the need of taking into account the soil collapse to predict correctly settlement subsidence and profile in a tunnel excavated in porous collapsible soil.

## 6 CONCLUSION

A preliminary analysis of the Brasilia subway tunnel was executed, using a new version of the Modified Cam-Clay Model. It was determined that the support pressure is around 38% of the initial stresses, in other words, it is mobilised after 62% of stress relief. It was demonstrated that soil collapse must be taken into account to predict correctly the settlement subsidence and profile, especially the elevated values at the surface. The magnitude of the settlements due to collapse is strongly dependent on the soil stiffness reduction after collapse and the extent of the collapsible zone. The collapse criterion seems to be associated to the occurrence of an extension zone above the tunnel, that causes the failure of the weak cementation links of the porous clay.

## REFERENCES

- CORDING, E.J. & HANSMIRE, W.H. (1975). "Displacements around Soft Ground Tunnels". 5<sup>th</sup> Copa MSEF, Vol. IV, pp. 571-633, Buenos Aires.
- DUNCAN, J.M. & CHANG, C.Y. (1970). "Nonlinear Analysis of Stress and Strain in Soils". J. Soil Mech. Fnds., ASCE, Vol. 96, pp. 1629-1653.
- FARIAS, M.M. (1993). "Numerical Analysis of Clay Core Dams". PhD thesis, University of Wales, Swansea, UK.
- NAYLOR, D.J. (1994). "Constitutive Laws for Static Analysis of Embankment Dams". Proc. of the 1<sup>st</sup> International Workshop on Applications of Computational Mechanics in Geotechnical Engineering, pp. 289-316, Rio de Janeiro, Brazil, July of 1991.
- NAYLOR, D.J. & MARANHA, J. (1992). "Influence of Stress Path on Collapse Settlement". Internal Report, University of Wales, Swansea, UK.
- NAYLOR, D.J., PÁNDE, G.N., SIMPSON, B. & TABB, R. (1981). "Finite Elements in Geotechnical Engineering". Pineridge Press, Swansea, UK.

- NAYLOR, D.J., FARIAS, M.M. & MARANHA, J. (1993). "Load Transfer in Central Core Dams due to Differential Settlement". International Workshop on Dam safety Evaluation, Switzerland, pp. 71-82.
- NAYLOR, D.J., TONG, S.L. & AMIR SHAHKARAMI, A. (1989). "Numerical Modelling of Saturation Shrinkage". Numerical Models in Geomechanics (NUMOG III), pp 636-648.
- NOBARI, E.S. & DUNCAN, J.M. (1972). "Movements in Dams due to Reservoir Filling". Special Conference on Performance of Earth-Supported Structures, Vol. 1, Part 1, pp. 797-815, Purdue University. ASCE.
- ORTIGÃO, J.A.R. & MACEDO, P. (1993). "Large Settlements due to Tunneling in Porous Clay". Tunnels et Ouvrages Souterrains, Paris, Vol. 119, pp. 245-290.
- PECK, R.B. (1969). "Deep Excavations and Tunneling in Soft Ground". Proc. 7th ICSMFE, pp. 225-290, Mexico.
- TONG, S.L. (1992). "Numerical Modelling of the Performance of Embankment Dams". PhD thesis, University of Wales, Swansea, UK.